Tetrahedron xxx (2018) 1–8

Contents lists available at ScienceDirect

Tetrahedron

journal homepage: www.elsevier.com/locate/tet

Cascade reactions leading to the mechanism of action of vinaxanthone and xanthofulvin, natural products that drive nerve repair

Anders M. Eliasen [a], Matthew R. Chin [b], Abram J. Axelrod [c], Ruben Abagyan [d], Dionicio Siegel [d, *]

[a] California Institute for Biomedical Research, La Jolla, CA 92037, USA
[b] Gilead Sciences, Inc., Foster City, CA 94404, USA
[c] Laboratory for Bioorganic Chemistry, Sloan-Kettering Institute for Cancer Center Research, New York, NY 10021, USA
[d] Skaggs School of Pharmacy and Pharmaceutical Sciences, University of California, San Diego, La Jolla, CA 92093, USA

ARTICLE INFO

Article history:
Received 5 January 2018
Received in revised form
23 February 2018
Accepted 27 February 2018
Available online xxx

Keywords:
Methodology
Total synthesis
Biosynthesis
Natural product
Regeneration
SUCNR1
Succinate receptor
Allosteric
GPCR

ABSTRACT

The natural products vinaxanthone and xanthofulvin promote regeneration in animal models of spinal cord injury and corneal transplant. However, inhibition of the initially described biological target of these compounds, semaphorin 3A, does not fully account for the recovery demonstrated *in vivo* following administration of the natural products. Through chemical synthesis substantial quantities of both natural products have been accessed with early reaction development paving the way for synthesizing both compounds. The success of a model system, first disclosed herein, translated to the syntheses of both natural products. Following from this we also report for the first time the discovery of a new target of the natural products, the succinate receptor 1 (SUCNR1). Both natural products function as positive allosteric modulators of SUCNR1. As the first known allosteric modulators of SUCNR1, the compounds represent powerful new tools to understand the pharmacology of SUCNR1 and its control of growth and cellular defense.

1. Introduction

It can be difficult to predict *in vitro in vivo* correlation (IVIVC) phenomena, as the transition from *in vitro* assays into preclinical testing frequently yields unforeseen effects. These effects can be increased toxicity, loss of activity, or only partial recapitulation of the effects based on the *in vitro* hypotheses. An additional, and highly desirable, phenomenon is enhancement of the expected phenotypic response through unforeseen synergistic off-target effects. However, deconvolution of these multiple effects is required to capitalize on these rare, serendipitous discoveries. We have found this is the case for the natural products vinaxanthone and xanthofulvin (Fig. 1), which induce a strong regenerative response in rodent models of spinal cord injury and corneal transplantation. Access to the compounds to permit this was achieved through reaction development that led to the creation of useful laboratory preparations, total synthesis.

Both natural products were initially identified as semaphorin 3A (Sema3a) inhibitors, capable of inhibiting the protein-protein interaction of Sema3a with its receptor, the plexin-neuropilin-1 complex.[1–3] Semaphorins have membrane-bound and soluble forms, are upregulated following injury to neurons in the central nervous system (CNS), and are found in high concentrations within fibroblasts at the site of injury.[4–6] Similar to other guidance cues, Sema3a plays an inhibitory role in axonal guidance, angiogenesis, and cellular movement. Towards validating the hypothesis that Sema3a inhibition provides a long sought target for CNS injury full spinal cord transection model in rats were examined with both natural products.[7,8] From these studies it was found that xanthofulvin and vinaxanthone enhance axonal regeneration, promote remyelination, increase angiogenesis, and attenuate lesion scarring. The combination of these effects leads to an improved functional recovery. Relatedly, administration of vinaxanthone following corneal transplant improved innervation into the transplanted

* Corresponding author.
E-mail address: drsiegel@ucsd.edu (D. Siegel).

https://doi.org/10.1016/j.tet.2018.02.068
0040-4020/

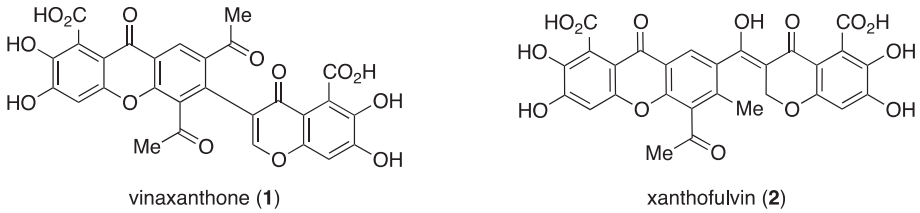

Fig. 1. Structures of vinaxanthone (**1**) and xanthofulvin (**2**).

tissue.[9] However, other Sema3a inhibitors do not elicit this type of response, suggesting unknown, positive off-target interactions. Additionally, advanced investigation into the effects of Sema3a on regeneration determined that decreased or absent Sema3a activity alone was not responsible for the diverse beneficial effects the compounds induced following spinal cord injury.[10] These findings taken together suggest other biological target(s) exist for vinaxanthone and xanthofulvin and that these are important components to the complete mechanism of action of these natural products.

2. Results and discussion

Initially, access to both vinaxanthone and xanthofulvin was limited to fermentation using *Penicillium* sp. SPF-3059, a fungus utilized by Sumitomo Dainippon Pharma. A laboratory preparation of vinaxanthone was reported in 2007, however, a late stage Diels-Alder reaction with a concomitant oxidation/aromatization sequence in the synthesis proved variable and incompatible with analog synthesis and could not be utilized to access xanthofulvin.[11] To provide improved access our laboratory has developed a fully synthetic approach to both vinaxanthone and xanthofulvin.[12] Additionally, our synthetic platform can furnish analogues to interrogate the role of each carboxylic acid and phenol substituents in CNS tissue regeneration. This matrix of analogues has elucidated a greater understanding of structure features enabling damage repair.[13] Early studies surrounding the syntheses of the natural products were based on hypothetical dimerization-like reactions that were proposed to occur spontaneously with a non-enzymatic union of two simpler compounds to directly prepare the larger, targeted natural products proceeding through the proposed cascade sequence shown in Scheme 1.

Reaction development was inspired by the proposed cascade sequence and focused on the synthesis of triketone (**14**) as a simplified surrogate for dehydropolivione (**3**) (Fig. 2). This was required for optimization as using the highly polar compound would provide a poor readout of reaction efficiency due to isolation/purification challenges. The synthesis of triketone **14** starting from vinylogous amide **15** required the introduction of an acetoacetate group, which was sought in a single operation (Scheme 2). The vinylogous amide (**15**) has two reactivity attributes as it serves as the framework to stitch the chromone ring together through direct acetoacetylation. The reaction was investigated using several acetoacylating reagents, acyl-ketene equivalents. Acyl transfer reaction onto enaminone **15** would first result in phenolic esterification, ester **17**, followed by spontaneous *O* → *C* transfer via the vinylogous amide acting as a nucleophile to furnish **20**, then after loss of dimethylamine the desired compound **14**.

This transformation was first attempted with diketene and only generated the expected product in 2% yield and proved unable to be improved (Entry 1, Table 1). However, triketone **14** was able to be characterized by single crystal x-ray diffraction and under these conditions it was shown to be in the enol form (Fig. 3). Given the low yield different acetoacetylation reagents were examined to improve the conversion of enaminone **15** to triketone **14**. Thermolysis of furan-dione (Entry 2) in toluene at reflux furnished

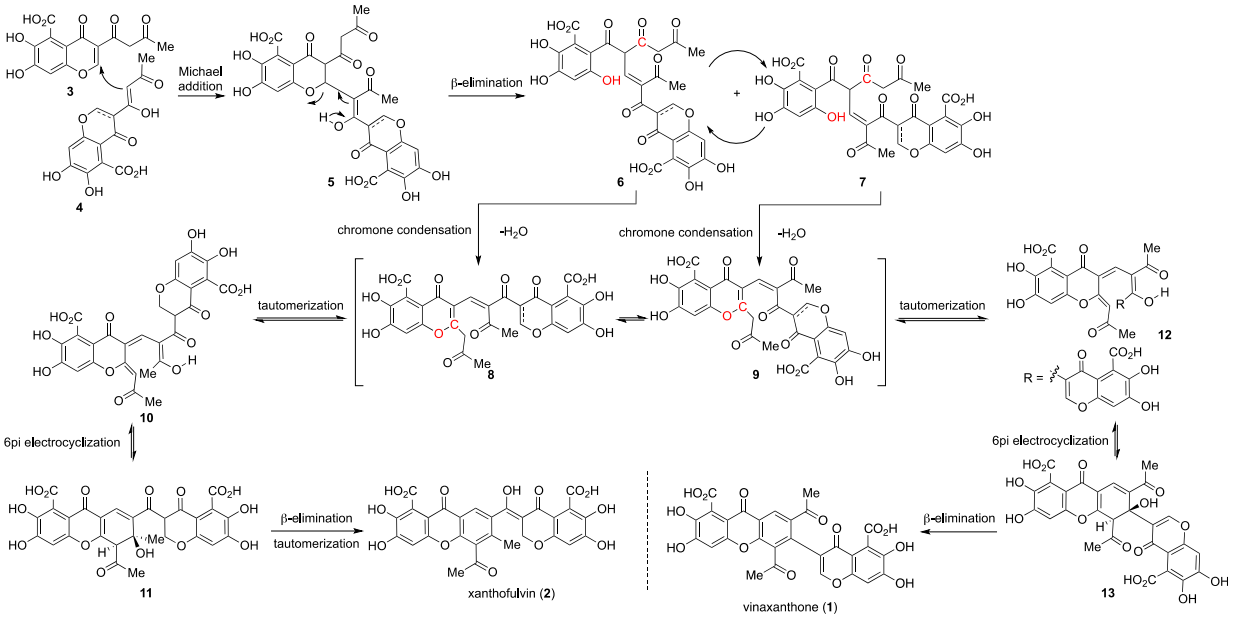

Scheme 1. Proposed biosynthesis of vinaxanthone (**1**) and xanthofulvin (**2**) through nonenzymatic, cascade reactions.

Please cite this article in press as: Eliasen AM, et al., Cascade reactions leading to the mechanism of action of vinaxanthone and xanthofulvin, natural products that drive nerve repair, Tetrahedron (2018), https://doi.org/10.1016/j.tet.2018.02.068

Fig. 2. Model system **14** of 5,6-dehydropolivione (**3**) for dimerization studies.

triketone, again in low yield. Exposure of enaminone **15** to commercially available dioxinone (Entry 3) provided triketone **14** in 11% yield, which was an improvement but still not useful for the process we sought to develop. Acyl Meldrum's acid (Entry 4 and 5) underwent thermolysis in the presence of enaminone **15** and the yield was increased to 16%. Optimization of this result led to an enhanced protocol utilizing a pre-heated oil bath at 145 °C ensuring near immediate acyl ketene generation, and purification with phosphoric acid-treated (pH = 2) silica gel, which provided triketone **14** in a reproducible 43% yield.

Hoye and co-workers had studied the chemistry of thioacetoacetates as acyl ketene donors, which can react under mild ambient conditions in the presence of a thiophilic silver salt.[14] Under this protocol (Entry 6, Table 1) a yield of 67% was achieved improving from the previous reactions. Attempts to optimize this further were not met with success, but the reaction was capable of good material throughput.

With access to triketone **14** the proposed dimerization reaction (Scheme 1) was made possible. Testing solvents and combinations, without added acid or base, quickly arrived at the ideal solvent system; a heated mixture of water/dioxane which cleanly furnished the cyclized, dimerized adduct **21**, assembling the carbogenic scaffold of vinaxanthone in a single reaction from **14** (Table 2). The structure of **21** was confirmed using 2D-NMR analysis. Noteworthy, the reaction proceeds under neutral conditions and the addition of acids or bases were deleterious, as an example treatment under basic conditions with triethylamine furnished the hydroxylated benzophenone **22** rather than the desired xanthone.

Using the methodological finding of the facile dimerization applying it to the synthesis of vinxanthone required the synthesis of the hypothetical natural product precursor 5,6-dehydropolivione (**3**). Starting from tetronic acid (**23**) 5,6-dehydropolivione was synthesized in eight steps (Scheme 3). Minor modification to the reaction conditions used in the model system, namely replacing the binary solvent system with water alone and lowering the temperature (and extending the reaction time) the natural product vinaxanthone was accessed for the second time by chemical synthesis, the first was achieved in 2007[11] using Diels-Alder chemistry. Our nine-step synthesis generated ample material for testing.

However, the application of this reaction to the synthesis of xanthofulvin following from a postulated reaction of 5,6-dehydropolivione and polivione (**24**) failed, only generating vinaxanthone regardless of addition sequences, stoichiometery and a variety of other perturbations of the previously successful method (Scheme 4). While this reaction did not translate it did provide insight into the appropriate synthetic approach toward xanthofulvin, namely the two partners needed to have singular reactivity i.e. Michael donor or Michael acceptor, not both types of reactivity as 5,6-dehydropolivione demonstrates.

Using a surrogate for dehydropolivione, an ynone such as **25** that can only function as a Michael acceptor provided a promising subtarget. A proposed conjugate addition into the ynone **25** by a ketoester would proceed through a related series of reactions to form the xanthone core of xanthofulvin (Fig. 4). Previously this type of reactivity had been documented with 3-(1-alkynyl)chromones and 1,3-dicarbonyl compounds under basic conditions providing support for our approach.[15]

The subtarget ynone **33** was prepared in nine steps from tetronic acid using a similar synthetic pathway as developed for 5,6-dehydropolivione (**3**) (Scheme 5). The addition of the sodium anion of methyl acetoacetate, using sodium hydride, formed the xanthone core in a single operation yielding xanthone **34**. With access to **34** the preparation of xanthofulvin required an additional five synthetic steps. This provided the first synthesis of xanthofulvin. In addition to providing synthetic material for the first time the synthesis resolved an inconsistency in the literature regarding an alternative structural assignment of xanthofulvin as a proposed structure dubbed 411J.[16]

With scalable access to both natural products, enabled by the methods development, the evaluation of the mechanism of action beyond Sema3a inhibition was made possible. Previously, the pharmacological profile of vinaxanthone and xanthofulvin against panels of enzymes and kinases was examined showing a high level of selectivity for Sema3a.[7,8] Given the dual anionic nature of the compounds at physiological pH, it was expected that the molecules would not readily enter cells. Accordingly, we investigated different cell surface proteins as potential targets using the previously utilized concentrations of the natural products, 0.2 μM. Through these studies commercial panel of 165 G-protein coupled receptors (GPCRs) were assayed for activity against vinaxanthone and xanthofulvin. It is noteworthy that both compounds failed to function as agonists nor antagonists for any of the GPCRs examined. However, it was found that both compounds markedly enhance the affinity and efficacy of succinate receptor 1 (SUCNR1) towards its ligand succinate although both natural products demonstrate no agonistic activity. (Fig. 4).

Studies into SUCNR1 evolved rapidly following the discovery in 2004 that the then orphaned GPCR, GPR91, was activated by succinate at concentrations of 56 ± 8 μM (aequorin assay) and 28 ± 5 μM (FLIPR assay).[17] Activation by succinate occurs due to increased concentration of succinate, relative to a baseline of 2–20 μM in different tissues, [18,19] This in turn leads to transcription of factors enabling angiogenesis and growth. This response occurs at lower concentration than that required for succinate stabilization of hypoxia inducible factor (HIF), providing evidence that many of the effects of succinate that have been linked to HIF in fact may be due to activation of SUCNR1.[20] Since both the neuronal and vascular system share similar signaling pathways, production of growth factors not only leads to enhanced blood vessel development but also to heightened axonal growth.[21] The activation of SUCNR1 leads to the pronounced growth promoting effects seen

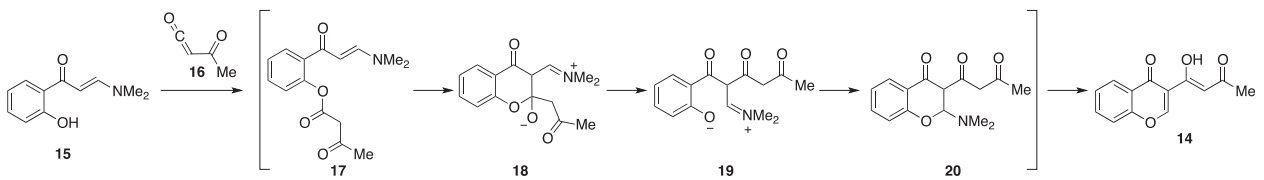

Scheme 2. Proposed cascade reaction of enamine **15** with acylketene (**16**) to generate triketone **14**.

Please cite this article in press as: Eliasen AM, et al., Cascade reactions leading to the mechanism of action of vinaxanthone and xanthofulvin, natural products that drive nerve repair, Tetrahedron (2018), https://doi.org/10.1016/j.tet.2018.02.068

Table 1
Reaction of enaminone **15** with compounds that can generate acylketene to form triketone **14**.

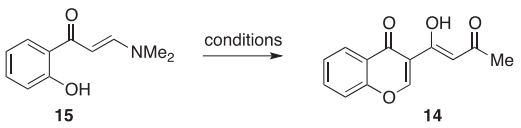

entry	reagents	Solvent/temp.	yield
1.		PhMe, 110 °C	2%
2.	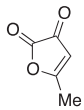	PhMe, 110 °C	3%
3.	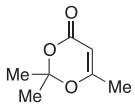	PhMe, 110 °C	11%
4.	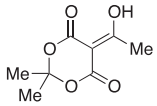	PhMe, 110 °C	16%
5.	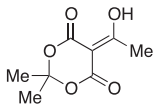	PhMe, 110 °C rapid heating	43%
6.	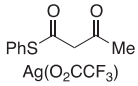	CH_2Cl_2, 23 °C	67%

Table 2
Dimerization reactions of **14** to form the polycyclic core of vinaxanthone **21**.

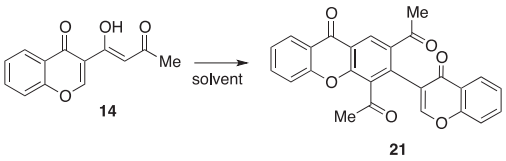

entry	Solvent/temp.	yield
1	dioxane, 90 °C	0%
2.	H_2O: dioxane, 100 °C	72%
3.	HCO_2H: dioxane, 90 °C	73%
4.	Et_3N, MeCN, 23 °C	42%

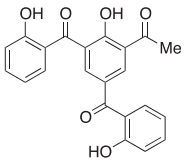

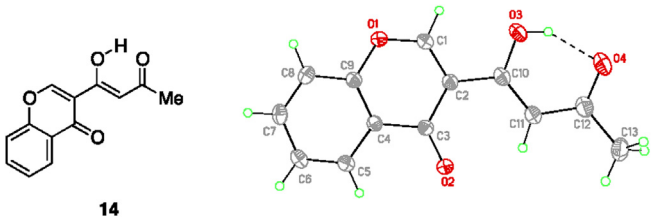

Fig. 3. X-ray crystal structure of the enol form of triketone **14**.

with vinaxanthone and xanthofulvin by enhancing the intrinsic growth potential of the neurons, simultaneously aiding in tissue repair and increased angiogenesis. In a rarity among receptors, both VEGF and Sema3a are agonists for the same cellular receptor neuropilin-1! However, the downstream effects of these signaling molecules contrast one another. Thus, activation of SUCNR1 indirectly opposes the action of Sema3a by stimulating the formation of vascular endothelial growth factor (VEGF).[22,23]

To develop a model for the binding of the natural products CR the sequence of the succinate receptor was searched against all GPCRs in the Protein Data Bank and the two candidate templates for homology modeling were identified: P2Y purinoceptor 1 (P2Y1) (pdb code 4xnv), and fractalkine receptor (pdb code 4xt3). After removal of the extra domains grafted to assist crystallization, the two proteins were structurally superimposed and an alignment was generated based on the structural superposition. The alignment shows only 25% sequence identity and the superposition shows overall topological similarities with significant deviations in a number of regions.

One major structural difference is centered around the extracellular loop 2 (ECL2) (magenta on Fig. 5A). Despite identical loop length, ECL2 is shallower in the fractalkine receptor structure but descends into the ligand binding pocket of the P2Y1 receptor in a much deeper fashion. That became the reason for, after performing all calculations with both models, dropping the P2Y1-based SUCR1 models and continuing only with the fractalkine receptor-based models.

After building and refining the homology model of ligand-free SUCR1, the binding pose of succinate was obtained by docking charged succinate into the flexible pocket area around the central extracellular cavity of the SUCR1 model. The following side chains were fully flexible: Y30, Y83, R99, L102, H103, L106, E153, Y187, S188, L191, Y248, H249, R252, R255, Y277, R281. Ten million iterations of the global optimization were performed with the Internal

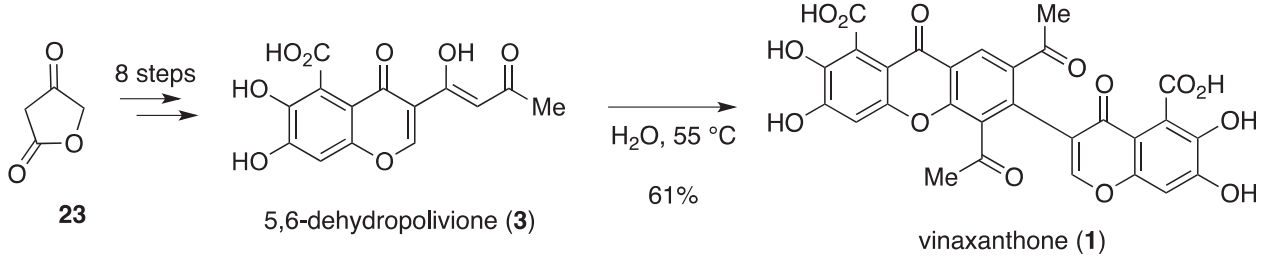

Scheme 3. Access to 5,6-dehydropolivione (**3**) from teronic acid (**23**) and dimerization of 5,6-dehydropolivione (**3**) to generate vinaxanthone (**1**).

Please cite this article in press as: Eliasen AM, et al., Cascade reactions leading to the mechanism of action of vinaxanthone and xanthofulvin, natural products that drive nerve repair, Tetrahedron (2018), https://doi.org/10.1016/j.tet.2018.02.068

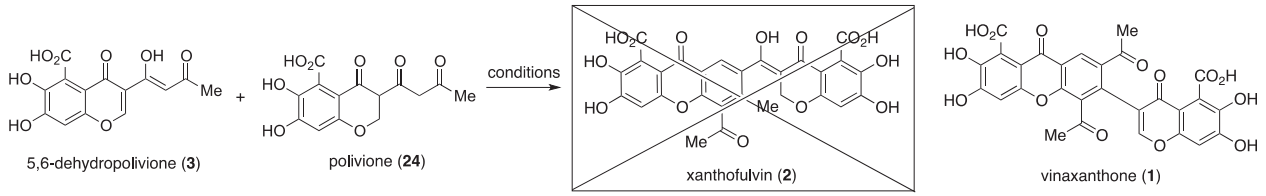

Scheme 4. Failed cross-reaction for the synthesis of xanthofulvin (**2**) using 5,6-dehydropolivione (**3**) and polivione (**24**) instead generating vinaxanthone (**1**).

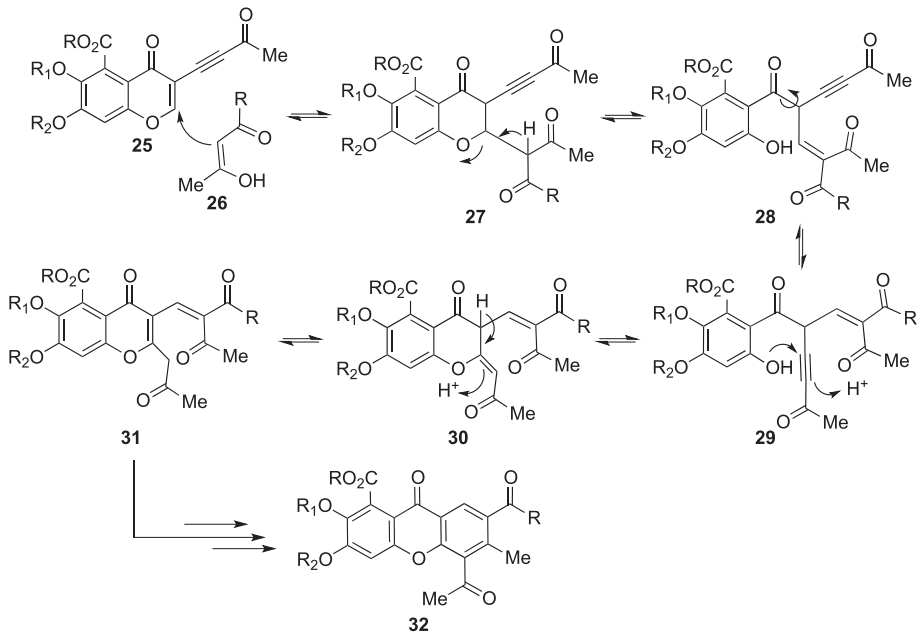

Fig. 4. Proposed coupling of a defined Michael acceptor, ynone **25** with a 1,3-dicarbonyl partner **26**.

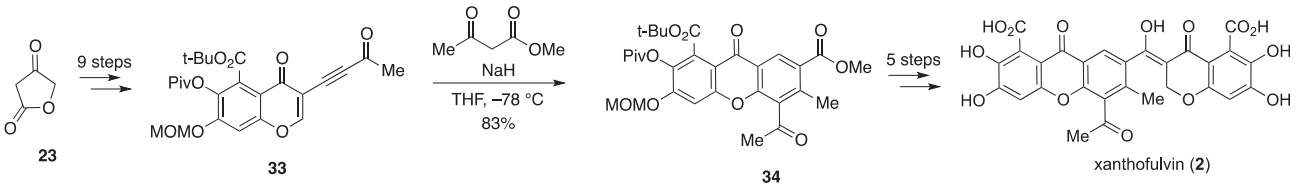

Scheme 5. Successful synthesis of xanthofulvin (**2**) using ynone **33** as a defined Michael acceptor. Elaboration of xanthone **34** over 5 steps provided synthetic xanthofulvin for the first time.

Coordinate Mechanics (ICM) program by concurrent stochastic docking of flexible succinate and sampling of the side chains.[24–26] The lowest energy conformation is shown on Fig. 6. In accordance with the mutation data, the docked succinate is hydrogen bonded to Arg99, His103, Arg252 or Arg281 while R255, His249 and Tyr107 are outside of the interaction area.

Our hypothesis is based on detailed analysis of the binding pocket, we found a large space above the bound succinate that was large enough to accommodate both vinaxanthone and xanthofulvin. To validate the hypothesis, the flexible models of these two positive allosteric modulators of SUCR1 were docked to the flexible pocket of the model with the bound succinate. The pockets appeared to have very close complementarity to both modulators, with the docked poses shown (Fig. 7A and B). According to the model, both vinaxanthone and xanthofulvin form an almost perfect lid for succinate thus, apparently, preventing it from leaving.

3. Conclusion

Reaction development has provided access to vinaxanthone and xanthofulvin providing the material that has been used for identifying their new biological targets. The cascade reactions provided a means for the synthesis of vinaxanthone through a dimerization reaction and allowed the synthesis of the core of xanthofulvin. With experimental, possible through total synthesis, and computational support of vinaxanthone and xanthofulvin functioning as positive allosteric modulators for SUCNR1 a more complete understanding of how the natural products promote regeneration has been developed. Future studies to identify if both Sema3a inhibition and SUCNR1 modulation are required for regeneration or if the growth response occurs solely by SUCNR1 activation are logical progressions given the findings reported herein. In addition, as the compounds function as the first known PAMs of SUCNR1 new chemical tools to study this receptor are now available.[27]

Please cite this article in press as: Eliasen AM, et al., Cascade reactions leading to the mechanism of action of vinaxanthone and xanthofulvin, natural products that drive nerve repair, Tetrahedron (2018), https://doi.org/10.1016/j.tet.2018.02.068

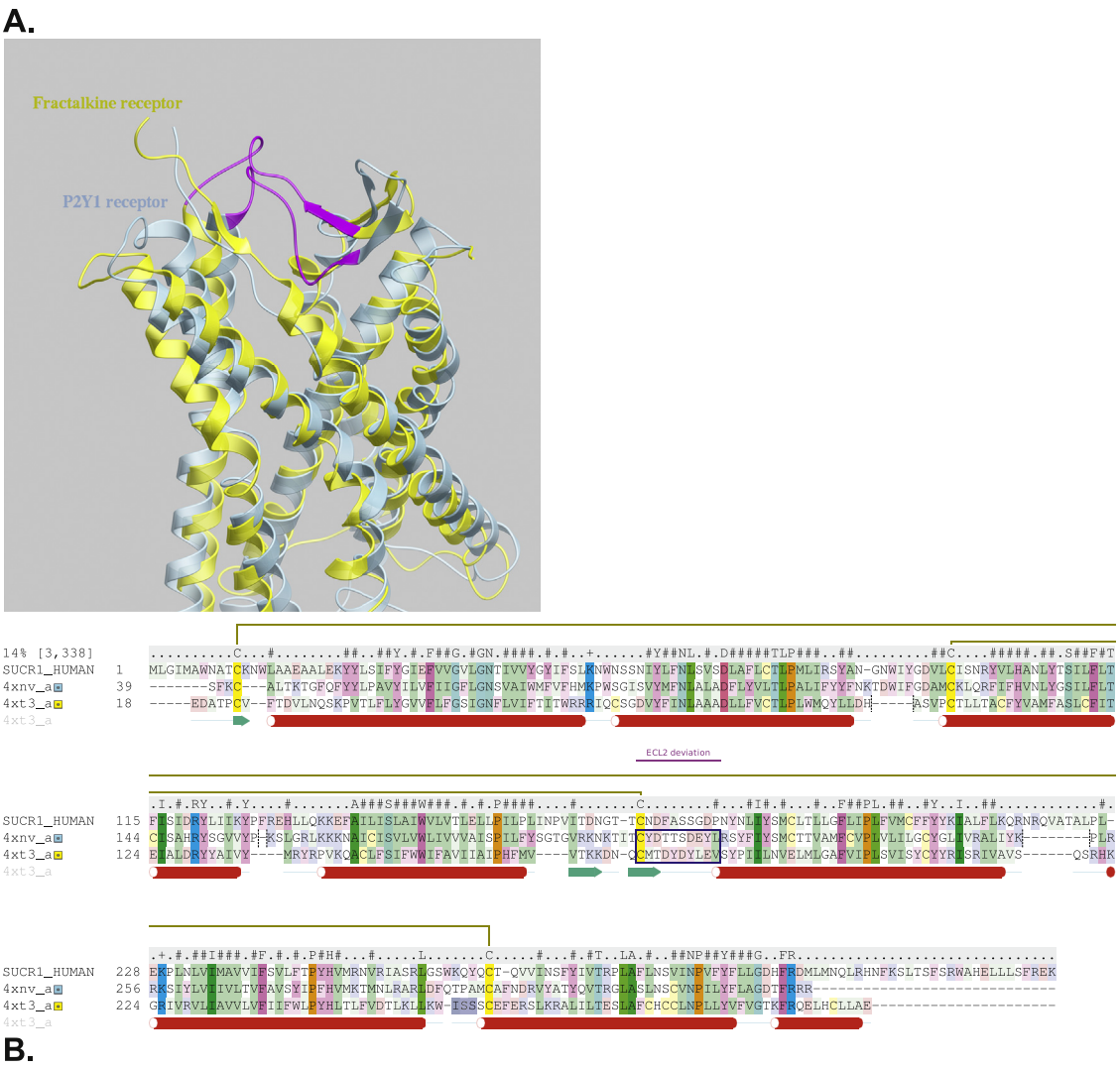

Fig. 5. A. The superposition of two homology modeling templates for the succinate receptor Note deviations of ECL2 and helix 5. The fractalkine receptor (yellow ribbon) has a more open conformation of the ECL2 (shown in magenta on both receptors). **B.** The structural alignment of the two receptors with determined three-dimensional structure was a guide for the alignment of the succinate receptor sequence. ECL2 is shown by a blue box. Combined with the SUCR1 alignment to both of them.

4. Experimental section

Organic solutions were concentrated by rotary evaporation at ~20 torr. Methylene chloride (CH_2Cl_2), diethyl ether (Et_2O), tetrahydrofuran (THF) and toluene (PhMe) were purified using a Pure-Solv MD-5 Solvent Purification System (Innovative Technology). All other reagents and solvents were used directly from the supplier without further purification. Analytical thin-layer chromatography (TLC) was carried out using 0.2 mm commercial silica gel plates (silica gel 60, F254, EMD chemical) and visualized using a UV lamp. TLC plates were stained using ceric ammonium molybdate (CAM), aqueous potassium permanganate ($KMnO_4$) or iodine. Infrared spectra were recorded on a Nicolet 380 FTIR using neat thin film technique. High-resolution mass spectra (HRMS) were recorded on a Karatos MS9 and are reported as *m*/*z* (relative intensity). Accurate masses are reported for the molecular ion $[M+Na]^+$, [M+H], $[M^+]$, or [M-H]. Nuclear magnetic resonance spectra (^1H NMR and ^{13}C NMR) were recorded with a Varian Mercury 400 (400 MHz, ^1H at 400 MHz, ^{13}C at 100 MHz), Agilent MR 400 (400 MHz, ^1H at 400 MHz, ^{13}C at 100 MHz), Varian DirectDrive 400 (400 MHz, ^1H at 400 MHz, ^{13}C at 100 MHz), or Varian DirectDrive 600 (600 MHz, ^1H at 600 MHz, ^{13}C at 150 MHz). For $CDCl_3$ solutions the chemical shifts are reported as parts per million (ppm) referenced to residual protium or carbon of the solvent: δ H (7.26 ppm) and δ C (77.0 ppm). Coupling constants are reported in Hertz (Hz). Data for ^1H NMR spectra are reported as follows: chemical shift (ppm, referenced to protium; s = singlet, d = doublet, t = triplet, q = quartet, p = pentet, sext = sextet, sept = septuplet, dd = doublet of doublets, td = triplet of doublets, ddd = doublet of doublet of doublets, m = multiplet, coupling constant (Hz), and integration). Melting points were measured on a MEL-TEMP device without corrections.

4.1. (E)-3-(dimethylamino)-1-(2-hydroxyphenyl)prop-2-en-1-one 15

O-hydroxy acetophenone (3.0 g, 22.0 mmol, 1.0 equiv.) and dimethylformamide dimethylacetal (8.81 mL, 66.1 mmol, 3.0 equiv.) were combined in dimethoxyethane (44.1 mL). The colorless solution heated to 85 °C and after 5 h the red homogeneous solution was concentrated *in vacuo* to afford **15** as a solid (4.18 g,

Please cite this article in press as: Eliasen AM, et al., Cascade reactions leading to the mechanism of action of vinaxanthone and xanthofulvin, natural products that drive nerve repair, Tetrahedron (2018), https://doi.org/10.1016/j.tet.2018.02.068

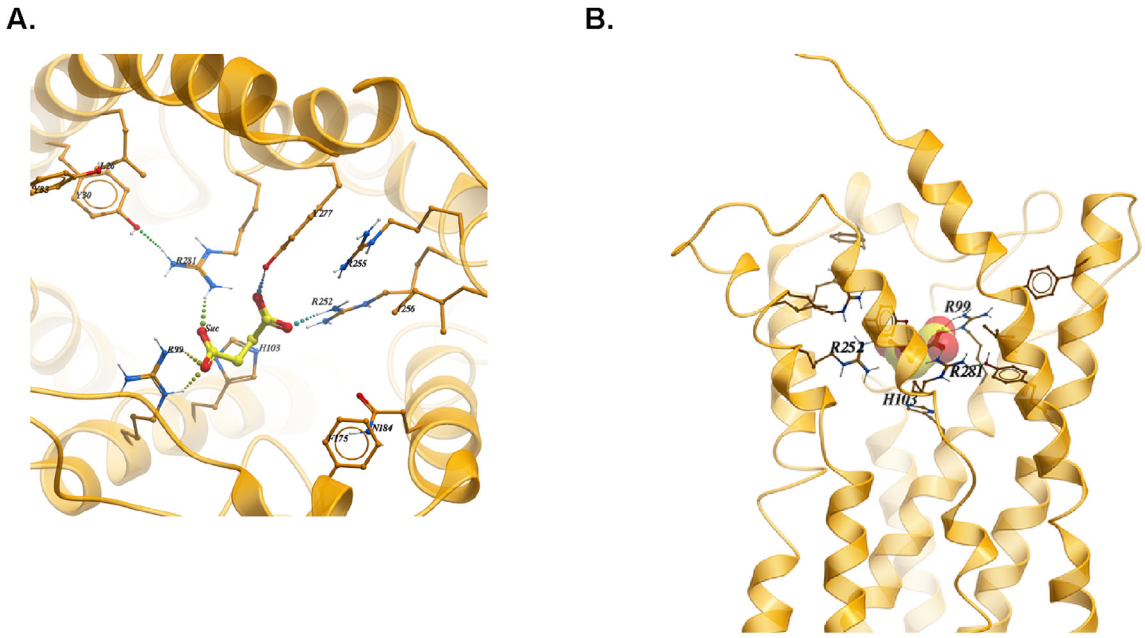

Fig. 6. The predicted model of the succinate bound to the Succinate receptor based on stochastic simulation of flexible receptor pocket. The top view (A) is the view from the extracellular compartment; side view (B) shows the view parallel to the membrane. The predicted hydrogen bonds are shown.

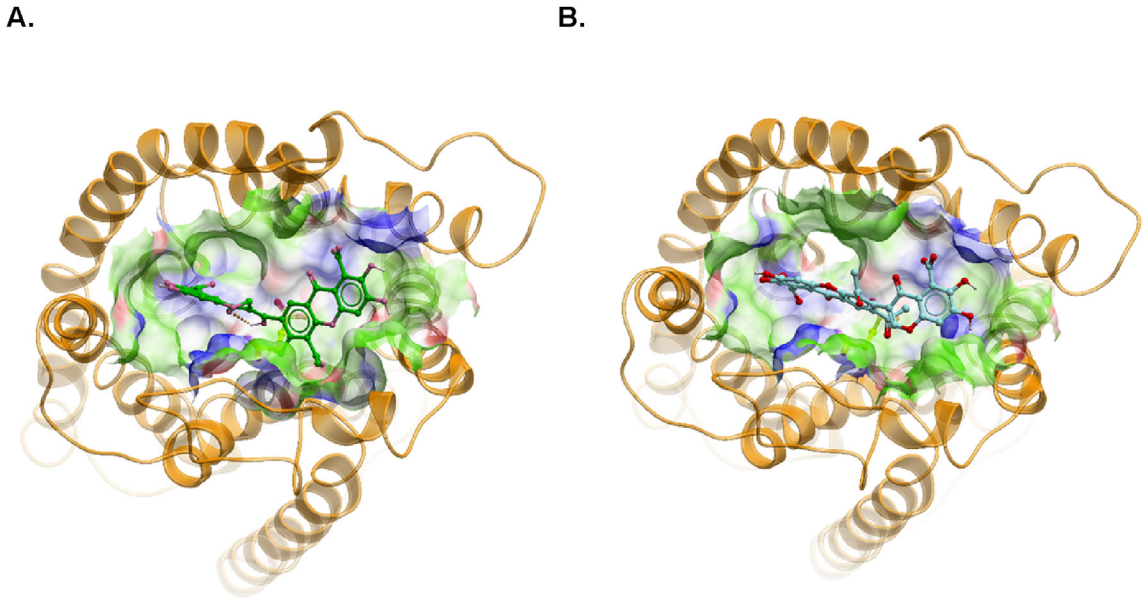

Fig. 7. The predicted poses of vinaxanthone (**A**) and xanthofulvin (**B**) covering the bound succinate like a lid (top view from the extracellular space). The carbons of the succinate appear to be in direct contact with the ligands.

21.9 mmol, 99% yield).

Golden solid, M.P. = 128–129 °C; $\mathbf{R_f}$ = 0.24 (silica gel, 1:1 hexanes: EtOAc); **^{1}H-NMR** (400 MHz, $CDCl_3$) δ 7.89 (d, J = 12.0 Hz, 1H), 7.69 (dd, J = 7.9, 1.7 Hz, 1H), 7.35 (ddd, J = 8.6, 6.8, 1.7, 1H), 6.84 (dd, J = 8.2, 1.0 Hz, 1H), 6.81 (ddd, J = 7.9, 6.8, 1.0 Hz, 1H), 5.79 (d, J = 12.3 Hz, 1H), 3.20 (s, 3H), 2.98 (s, 3H); **^{13}C-NMR** (100 MHz, $CDCl_3$) δ 191.3, 162.8, 154.7, 133.8, 128.2, 120.2, 118.0, 117.9, 89.8, 42.3, 37.3; **IR** (film, cm $^{-1}$) 1633, 1585, 1544, 1368; **HRMS** (ESI) calcd. for $C_{11}H_{14}NO_2$ $[M+H]^+$: 192.10191, obs. 192.10219.

4.2. (Z)-3-(1-hydroxy-3-oxobut-1-en-1-yl)-4H-chromen-4-one 14

To a stirred solution of enaminone **15** (50.0 mg, 0.261 mmol, 1.0 equiv.) and silver trifluoroacetate (57.8 mg, 0.261 mmol, 1.0 equiv.) in dichloromethane (2.60 mL) was added neat phenyl thioacetoacetate (78.0 μL, 0.261 mmol, 1.0 equiv.). The flask was protected from light and the heterogeneous solution was stirred for 48 h at ambient temperature. The reaction was the diluted with chloroform, passed through a pad of celite, and concentrated. The resulting orange semisolid was purified using acidified silica gel* and 7:1 hexanes: EtOAc as the eluent to afford **14** as a white solid (40.0 mg, 0.174 mmol, 67% yield).

Please cite this article in press as: Eliasen AM, et al., Cascade reactions leading to the mechanism of action of vinaxanthone and xanthofulvin, natural products that drive nerve repair, Tetrahedron (2018), https://doi.org/10.1016/j.tet.2018.02.068

White solid, M. P. = 142–144 °C; $\mathbf{R_f}$ = 0.33 (silica gel, 3:1 hexanes: EtOAc); **^{1}H-NMR** (400 MHz, $CDCl_3$) δ 15.90 (s, 1H), 8.78 (s, 1H), 8.28 (dd, J = 8.2, 1.7 Hz, 1H), 7.73 (ddd, J = 8.5, 7.2, 1.7 Hz, 1H), 7.52 (d, J = 8.5 Hz, 1H), 7.49 (ddd, J = 8.2, 7.2, 1.0 Hz, 1H), 7.12 (s, 1H), 2.24 (s, 3H); **^{13}C-NMR** (100 MHz, $CDCl_3$.) δ 224.3, 197.4, 174.7, 160.3, 155.5, 134.2, 126.3, 126.1, 124.5, 118.2, 118.1, 101.5, 26.7; **IR** (film, cm $^{-1}$) 3420, 1651, 1617, 1465; **HRMS** (ESI) calcd. for $C_{13}H_{10}NaO_4$ $[M+Na]^+$: 253.04713, obs. 253.04722.

*To a 4 L Erlenmeyer flask was added 400 g of silica gel. Added was 2.50 L of deionized water and the slurry stirred vigorously. The solution was acidified to a pH of 2 with 6.50 mL of 85% phosphoric acid. The slurry stirred for 20 min. The silica gel was filtered and washed with ethyl acetate, then dried in a 120 °C oven overnight.

4.3. (Z)-3-(1-hydroxy-3-oxobut-1-en-1-yl)-4H-chromen-4-one 14

Enaminone **15** (3.0 g, 15.7 mmol, 1.0 equiv.) and freshly ground acyl Meldrum's acid (8.76 g, 47.1 mmol, 3.0 equiv.) were dissolved in toluene (157 mL) and the solution was heated to reflux for 45 min. Removal of the volatiles yielded a brown semisolid. The crude material was purified using acidified silica gel* and 7:1 hexanes: ethyl acetate as the eluent to afford **14** as a white solid (1.55 g, 6.73 mmol, 43%).

White solid, M. P. = 142–144 °C; $\mathbf{R_f}$ = 0.33 (silica gel, 3:1 hexanes: EtOAc); **^{1}H-NMR** (400 MHz, $CDCl_3$) δ 15.90 (s, 1H), 8.78 (s, 1H), 8.28 (dd, J = 8.2, 1.7 Hz, 1H), 7.73 (ddd, J = 8.5, 7.2, 1.7 Hz, 1H), 7.52 (d, J = 8.5 Hz, 1H), 7.49 (ddd, J = 8.2, 7.2, 1.0 Hz, 1H), 7.12 (s, 1H), 2.24 (s, 3H); **^{13}C-NMR** (100 MHz, $CDCl_3$.) δ 224.3, 197.4, 174.7, 160.3, 155.5, 134.2, 126.3, 126.1, 124.5, 118.2, 118.1, 101.5, 26.7; **IR** (film, cm $^{-1}$) 3420, 1651, 1617, 1465; **HRMS** (ESI) calcd. for $C_{13}H_{10}NaO_4$ $[M+Na]^+$: 253.04713, obs. 253.04722.

*To a 4 L Erlenmeyer flask was added 400 g of silica gel. Added was 2.50 L of deionize d water and the slurry stirred vigorously. The solution was acidified to a pH of 2 with 6.50 mL of 85% phosphoric acid. The slurry stirred for 20 min. The silica gel was filtered and washed with ethyl acetate, then dried in a 120 °C oven overnight.

4.4. 1,1'-(9-oxo-3-(4-oxo-4H-chromen-3-yl)-9H-xanthene-2,4-diyl)diethanone 21

Acetoacetyl chromenone **14** (32.5 mg, 0.141 mmol) was stirred in a 1:1 mixture of water and dioxane (1.4 mL) heated to 100 °C for 14 h. The reaction was concentrated *in vacuo* to produce a yellow solid, which was purified by silica gel column chromatography using 99:1 dichloromethane: methanol to afford **21** (21.7 mg, 0.051 mmol, 72% yield).

White solid; M.P. = 264 °C; $\mathbf{R_f}$ = 0.35 (silica gel, 1:1 hexanes: EtOAc); **^{1}H-NMR** (400 MHz, $CDCl_3$) δ 8.76 (s, 1H), 8.37 (dd, J = 7.8, 1.6 Hz, 1H), 8.22 (dd, J = 7.8, 1.6 Hz, 1H), 7.90 (s, 1H), 7.79 (ddd, J = 8.6, 7.1, 1.6 Hz, 1H), 7.73 (ddd, J = 8.6, 7.0, 1.6 Hz, 1H), 7.42–7.53 (m, 4H), 2.67 (s, 3H), 2.49 (s, 3H); **^{13}C-NMR** (100 MHz, $CDCl_3$) δ 201.4, 199.0, 175.7 (2 signals), 156.4, 155.7, 154.4, 153.3, 135.8, 135.7, 134.4, 134.2, 133.3, 127.6, 126.9, 126.3, 125.6, 125.2, 123.7, 121.7, 121.6, 121.0, 118.3, 118.1, 32.3, 28.9; **IR** (film, cm $^{-1}$) 1709, 1684, 1639, 1464; **HRMS** (ESI) calcd. for $C_{26}H_{16}NaO_6$ $[M+Na]^+$: 447.08391, obs. 447.08391.

4.5. (5-acetyl-4-hydroxy-1,3-phenylene)bis((2-hydroxyphenyl) methanone) 22

Acetoacetyl chromenone **14** (20.0 mg, 0.087 mmol, 1.0 equiv.) was taken up in acetonitrile (1.7 mL). Neat triethylamine (8.8 μL, 0.087 mmol, 1.0 equiv.) was added and the reaction stirred for 14 h at 23 °C. The crude material was concentrated *in vacuo* to produce an orange oil, which was purified 100:10:1 hexanes: ethyl acetate: acetic acid to afford **2.58** as a yellow oil (6.90 mg, 0.0183 mmol, 42% yield).

Yellow oil; $\mathbf{R_f}$ = 0.41 (3:1 hexanes: EtOAc); **^{1}H-NMR** (400 MHz, $CDCl_3$) δ 13.10 (s, 1H), 11.89 (s, 1H), 11.67 (s, 1H), 8.37 (d, J = 2.1 Hz, 1H), 7.93 (d, J = 2.1 Hz, 1H), 7.52–7.59 (m, 3H), 7.38 (dd, J = 7.9, 1.4 Hz, 1H), 7.10 (d, J = 7.5 Hz, 1H), 7.06 (d, J = 7.9 Hz, 1H), 6.93 (ddd, J = 8.2, 7.2, 1.0 Hz, 1H), 6.86 (ddd, J = 8.2, 7.2, 1.0 Hz, 1H), 2.76 (s, 3H); **^{13}C-NMR** (100 MHz, C_6D_6) δ 204.4, 199.4, 198.4, 164.0, 163.8, 162.3, 137.2, 136.7, 136.3, 134.5, 133.4, 132.8, 128.6, 128.5, 120.2, 119.5, 119.2, 119.1, 119.0, 118.9, 118.7, 25.9; **IR** (film, cm $^{-1}$) 3066, 1626, 1684, 1639, 1464; **HRMS** (ESI) calcd. for $C_{22}H_{16}NaO_6$ $[M+Na]^+$: 399.08391, obs. 399.08414.

Computational methods

The global optimization were performed with the Internal Coordinate Mechanics (ICM) program by concurrent stochastic docking of flexible succinate and sampling of the side chains as described in references.[24–26]

Acknowledgements

This work has been supported financially by the Welch Foundation (F-1694) and the NSF (CHE-1151708), which are gratefully acknowledged. The authors thank Brendan Duggan for assistance with NMR spectroscopy.

Appendix A. Supplementary data

Supplementary data related to this article can be found at https://doi.org/10.1016/j.tet.2018.02.068.

References

1. Kikuchi K, Kishino A, Konishi O, et al. *J Biol Chem*. 2003;278:42985–42991.
2. Kumagai K, Hosotani N, Kikuchi K, Kimura T, Saji I. *J Antibiot*. 2003;56:610–616.
3. Takahashi T, Fournier A, Nakamura F, et al. *Cell*. 1999;99:59–69.
4. Pasterkamp RJ, Giger RJ, Ruitenberg MJ, et al. *Mol Cell Neurosci*. 1999;13:143–166.
5. Pasterkamp RJ, Giger RJ, Verhaagen J. *Exp Neurol*. 1998;153:313–327.
6. Pasterkamp RJ, Anderson PN, Verhaagen J. *Eur J Neurosci*. 2001;13:457–471.
7. Kaneko S, Iwanami A, Nakamura M, et al. *Nat Med*. 2006;12:1380–1389.
8. Zhang L, Kaneko S, Kikuchi K, et al. *Mol Brain*. 2014;7:14.
9. Omoto M, Yoshida S, Miyashita H, et al. *PLoS One*. 2012;7, e47716.
10. Lee JK, Chow R, Xie F, Chow SY, Tolentino KE, Zheng BH. *J Neurosci*. 2010;30:10899–10904.
11. Tatsuta K, Kasai S, Amano Y, Yamaguchi T, Seki M, Hosokawa S. *Chem Lett*. 2007;36:10–11.
12. Axelrod A, Eliasen AM, Chin MR, Zlotkowski K, Siegel D. *Angew Chem Int Ed Engl*. 2013;52:3421–3424.
13. Chin MR, Zlotkowski K, Han M, et al. *ACS Chem Neurosci*. 2015;6:542–550.
14. May AE, Hoye TR. *J Org Chem*. 2010;75:6054–6056.
15. Zhao L, Xie F, Cheng G, Hu Y. *Angew Chem Int Ed Engl*. 2009;48:6520–6523.
16. Wrigley SKLMA, Gibson TM, Chicarelli-Robinson MI, Williams DH. *Pure Appl Chem*. 1994;66:2383–2386.
17. He WH, Miao FJP, Lin DCH, et al. *Nature*. 2004;429:188–193.
18. Kushnir MM, Komaromy-Hiller G, Shushan B, Urry FM, Roberts WL. *Clin Chem*. 2001;47:1993–2002.
19. Sadagopan N, Li W, Roberds SL, et al. *Am J Hypertens*. 2007;20:1209–1215.
20. Sapieha P, Sirinyan M, Hamel D, et al. *Nat Med*. 2008;14:1067–1076.
21. Carmeliet P, Tessier-Lavigne M. *Nature*. 2005;436:193–200.
22. Joyal JS, Omri S, Sitaras N, Rivera JC, Sapieha P, Chemtob S. *Acta Paediatr*. 2012;101:819–826.
23. Guttmann-Raviv N, Shraga-Heled N, Varshavsky A, Guimaraes-Sternberg C, Kessler O, Neufeld G. *J Biol Chem*. 2007;282:26294–26305.
24. Abagyan R, Totrov M, Kuznetsov D. *J Comput Chem*. 1994;15:488–506.
25. Abagyan R, Totrov M. *J Mol Biol*. 1994;235:983–1002.
26. Kufareva I, Handel TM, Abagyan R. *Meth Mol Biol*. 2015;1335:295–311.
27. Gilissen J, Jouret F, Pirotte B, Hanson J. *Pharmacol Ther*. 2016;159:56–65.